Author(s): S.J. Metcalf, Z. Tamainot-Telto, , R.E. Critoph

Article Title: Application of a compact sorption generator to solar refrigeration: Case study of Dakar (Senegal)

Year of publication: 2011

Link to published article:
http://dx.doi.org/10.1016/j.applthermaleng.2010.11.001

Application of a compact sorption generator to solar refrigeration: Case study of Dakar (Senegal)

S.J. Metcalf, Z. Tamainot-Telto[(1)], R.E. Critoph

Sustainable Energy Engineering and Design Research Group

School of Engineering, University of Warwick, Coventry CV4 7AL, UK

Abstract

The feasibility of applying a low cost plate heat exchanger solid sorption reactor to solar powered refrigeration is investigated. The proposed system is targeted at ice-making in developing countries for food preservation. The adsorption refrigeration machine employs the active carbon-ammonia working pair in both two-bed and four-bed regenerative systems. Driving heat is provided from standard flat plate and evacuated tube solar collectors. The cost of a one-off machine with four regenerative beds which could produce up to 1000 kg of ice per day in Dakar (Senegal) is estimated at €68,000.

Keywords

Active carbon, adsorption, ammonia, ice-making, refrigeration.

[(1)] Corresponding author: E-mail z.tamainot-telto@warwick.ac.uk - Tel. +44 24 76522108 – Fax +44 24 76418922

NOMENCLATURE

A	Surface area (m^2)
c	Specific heat ($J\ kg^{-1}\ K^{-1}$)
COP	Coefficient of performance
G	Solar radiation incident on collector ($W\ m^{-2}$)
H	Specific heat of sorption ($J\ kg^{-1}$)
k	Dubinin coefficient
m	Mass flow rate ($kg\ s^{-1}$)
M	Mass (kg)
n	Dubinin coefficient
Q	Heat (J)
$\dot{Q}$	Heat flux (W)
SCP	Specific cooling power ($W\ kg^{-1}$)
t	Thickness (m) ; Time (s)
T	Temperature (K)
U	Overall heat transfer coefficient ($W\ m^{-2}\ K^{-1}$)
x	Concentration (kg Ammonia kg^{-1} Carbon)

Greek letters

η	Efficiency
λ	Thermal conductivity ($W\ m^{-1}\ K^{-1}$)
Δ	Difference

Subscripts

a	Adsorbed phase
amb	Ambient
c	Carbon
col	Collector
cool	Cooling
f	Fluid (Liquid)
in	Inlet
LM	Log-Mean
o	Optical
out	Outlet
p	Pressure
sat	Saturation
v	Volume
w	Wall

Introduction

There is a large demand for cooling in developing countries in which there is no reliable electricity supply and fuels are difficult or too expensive too obtain. Such countries tend to receive high solar insolation, and so would appear to be ideal candidates for the application of solar refrigeration. The three main areas in which there is a demand for cooling are vaccine storage, food preservation and air conditioning. Research into solar powered solid sorption refrigeration systems has been active since the late 1970s. However, such systems have not been commercialised due to their high capital cost. For vaccine storage a high capital cost may be acceptable; however in food preservation or comfort air conditioning the capital costs must be reduced dramatically in order for such systems to become viable. Researchers at the University of Warwick have developed a prototype plate heat exchanger sorption generator for use in carbon-ammonia adsorption systems. This sorption generator is designed to increase specific cooling power (SCP, the cooling power per unit mass or volume of machine) in order to reduce capital costs and make such systems commercially viable [1, 2]. The sorption generator model has been validated against experimental data from both a car air conditioning system driven by waste heat from the engine coolant [3] and a gas fired heat pump [4]. Therefore, it is possible to explore with confidence other sorption applications using the current model.

The city of Dakar and its surrounds hosts about 95% of the industrial fishery activities of Senegal (West Africa) ranging from fish processing to ordinary stock storage for local consumption or exportation. Both artisanal and industrial fishery activities count for about 2.5% of GDP. The sector provides about 600,000 jobs and the fish contributes up to 70% of animal protein consumption (26 kg per person, per year) [5, 6]. In 2005, the fish capture production was estimated to be about 400,000 tonnes with 30% for export with a value of about €270M representing around 40% of the country's exports. The adsorption system is highly suited to application in remote areas and developing countries, as it contains relatively few moving parts and thus requires little maintenance. The adsorption system is driven by heat from conventional solar thermal collectors: the system could provide cooling requirements for fish preservation (typically 1 kg of ice per kg of fish) as sustainable technology that is complementary or a substitution to a conventional refrigeration machine. Furthermore such systems off-load the electrical grid since there is little or no electrical power requirement. This technology is suitable for both low cooling capacity (below 100 kg ice per day) and high cooling capacity (above 100 kg ice per day). The use of high pressure ammonia as the refrigerant is also favourable in comparison to sub-atmospheric water or methanol for which the ingress of air can be difficult to prevent.

This paper presents simulation results for the application of this low cost sorption generator to a solar powered refrigeration system. From weather data (mainly ambient temperature and solar insolation) provided by the Meteonorm package, simulations are carried out for a complete year for the city of Dakar and the cost of a solar sorption cooling system producing up to 1000 kg of ice per day is estimated.

Solar Refrigeration System

The proposed system consists of a multiple-bed regenerative adsorption system driven by heat from solar thermal collectors via a heat transfer fluid. Two solar collector types are considered: a flat plate type and an evacuated tube type, in order to compare their capital cost per unit cooling. Since the solar collector array is often the most significant part of the total system cost, the use of a standard solar collector should be the most cost effective solution. Details of the two types investigated are included in **Table 1**.

The adsorption system does not operate on a diurnal cycle as with most solar powered adsorption ice makers, but operates with a much shorter cycle time (circa 3 minutes) and produces ice during daylight hours. This minimises the size and therefore the cost of the adsorption system. Both a two-bed and a four-bed regenerative adsorption cycle with mass recovery are investigated. Although the four-bed cycle has a higher COP, SCP is lower and so a larger and thus more expensive machine is required. If the adsorption system cost were negligible in comparison to the solar collector cost then the four-bed system would always prove superior, since its higher efficiency would minimise the required collector area. However, the adsorption machine cost is unlikely to be negligible in all cases and therefore the economics of the two cycles needs to be investigated.

The plate heat exchanger sorption generator is shown in **Figure 1**. It is a prototype unit which is currently under development and is to be applied to adsorption systems for gas fired heat pumping and air conditioning and mobile air conditioning.

The unit is constructed from nickel brazed stainless steel and contains carbon adsorbent in 4 mm thick layers. The heat transfer fluid is pumped through chemically etched channels in the stainless steel shims which form the plates of the heat exchanger. The relatively thin layers of adsorbent and the large area for fluid heat transfer promote rapid temperature cycling and a high SCP. Similar units may be employed in the numerous applications outlined, thereby enabling economies of scale in their manufacture and further lowering the capital cost of the system.

The cost of such a heat exchanger is difficult to estimate at this early stage in its development. However, it seems reasonable to estimate it from the cost of an existing conventional plate heat exchanger with the same size and number of plates. The only conceivable additional cost involved in the manufacture of the unit would be that of the manufacture and insertion of the adsorbent. The cost of the carbon adsorbent itself will be negligible and the cost of adsorbent insertion in the heat exchanger will be considered negligible for the purposes of this analysis. **Table 2** gives the cost of a stainless steel brazed plate heat exchanger with plates of similar dimensions to the sorption generator, which will be used in the cost estimates.

Figure 2 present an example of a layout of solar powered sorption refrigeration system. The ammonia loop consists of a condenser, an expansion valve, an evaporator and a thermal compressor. This thermal compressor corresponds to two regenerative beds (with set of four check valve) and is driven by both solar collector and cooler.

System Performance Simulation

Sorption System Model

The sorption system model was created in MATLAB® and is a finite difference model. The schematic in **Figure 3** shows the configuration of the modelled generator bed. The adsorbent is in contact with a 'wall' that separates it from the heat transfer fluid, which facilitates the heat transfer to the adsorbent. The model contains two heat transfer coefficients – that between the fluid and the wall, and that between the wall and the carbon. Both the wall and adsorbent are isothermal, i.e. they are each modelled by a single lumped element.

The thermal resistance of the separating wall is considered negligible (since it is a highly conductive, thin metallic wall). The thermal contact resistance between the wall and the carbon is accounted for in the assumed value for the carbon thermal conductivity. The fluid-wall heat transfer coefficient was calculated from relationships given by Kays and London [7] for fully developed laminar flow in rectangular channels. The flow was confirmed as laminar by ensuring that the Reynolds number was less than the critical value. The wall-carbon heat transfer coefficient is calculated as

$$U_{wc} = \frac{2\lambda_c}{t_c} \tag{1}$$

Heat transfer between the fluid and the wall is calculated using a log mean temperature difference

$$\Delta T_{LMfw} = \frac{T_{fin} - T_{fout}}{ln\left(\dfrac{T_{fin} - T_w}{T_{fout} - T_w}\right)} \tag{2}$$

where ΔT_{LMfw} is the log-mean temperature difference between the heat transfer fluid and the wall. The governing equations for the model are:

$$M_w c_{pw} \frac{\partial T_w}{\partial t} = (UA)_{fw} T_{LMfw} - (UA)_{wc}(T_w - T_c) \tag{3}$$

$$M_f c_{pf} \frac{\partial T_f}{\partial t} - \dot{m} c_{pf}(T_{fin} - T_{fout}) = -(UA)_{fw} \Delta T_{LM\ fw} \tag{4}$$

$$M_c(c_{pc} + x c_{pa}) \frac{\partial T_c}{\partial t} - M_c H \frac{\partial x}{\partial t} = (UA)_{wc}(T_w - T_c) \tag{5}$$

In the model the fluid thermal mass is lumped with the wall thermal mass – an approximation in order to simplify the solution of the governing equations – so that equations (4) and (3) become equations (6) and (7) respectively.

$$\dot{m}c_{pf}(T_{fin} - T_{fout}) = (UA)_{fw}\Delta T_{LMfw} \tag{6}$$

$$(M_w c_{pw} + M_f c_{pf})\frac{\partial T_w}{\partial t} = (UA)_{fw}\Delta T_{LMfw} - (UA)_{wc}(T_w - T_c) \tag{7}$$

These equations are integrated through time using the explicit Euler scheme by substituting for $\partial x/\partial t$ in equation (5) with

$$\frac{\partial x}{\partial t} = \left(\frac{\partial x}{\partial T_c}\right)_P \frac{\partial T_c}{\partial t} \tag{8}$$

since in an idealised cycle adsorption and desorption occur at constant pressure. The concentration of adsorbed ammonia is calculated using a modified Dubinin-Astakhov equation [8]:

$$x = x_0\, exp(-K(T_c / T_{sat} - 1)^n) \tag{9}$$

and thus the first partial derivative on the RHS of equation (8) can be calculated analytically as

$$\left(\frac{\partial x}{\partial T_c}\right)_P = -\frac{Knx}{T_{SAT}}\left(\frac{T_c}{T_{SAT}} - 1\right)^{n-1} \tag{10}$$

The advantage of this simplified modelling approach is that results can be obtained quickly for a large number of cases. The stability and accuracy of the solutions was verified by varying the simulation time step by an order of magnitude and by manual checking of the temperature history for smoothness and signs of instability. The simulations were run for several temperature cycles until steady cyclic behaviour was obtained (usually after four cycles).

The sorption generator simulation parameters are given in **Table 3**. The adsorbent layer thickness, t_c, of 4 mm is half of the total layer thickness, since the other layer half will be heated and cooled via heat transfer fluid in the opposing plate. This is twice that of the layer thickness in the prototype shown in **Figure 1**. The layer thickness was increased in order to reduce the thermal mass of the generator (which was optimised for a mobile air conditioning application) and thereby increase COP. This reduces the required collector area. However, SCP and therefore the sorption generator cost are increased, and there is an optimum layer thickness dependent upon the relative cost of the collector and the sorption generator.

Sorption System Simulations

The sorption system model was used to calculate performance in terms of COP and SCP over a range of ambient temperatures and driving temperatures. The evaporating temperature was -5°C, selected as appropriate for ice production. The condensing temperature and the inlet temperature of the heat transfer fluid during final cooling of the sorption generators were assumed to be 5°C above ambient. **Figures 4** and **5** show the sorption system performance calculated from the model for driving temperatures between 65 and 245°C and ambient temperatures from 10 to 50°C for two and four-bed cycles, respectively.

<u>Solar Collector Calculations</u>

The efficiency of the solar collectors was calculated using the coefficients (linear loss coefficient, k_1 and quadratic loss coefficient, k_2) and optical efficiency (η_0) given in Table 1 in the following equation:

$$\eta = \eta_0 - k_1 \frac{(T_{col} - T_{amb})}{G} - k_2 \frac{(T_{col} - T_{amb})^2}{G} \tag{11}$$

The heat output from the solar collector is given by

$$\dot{Q}_{col} = \eta(T_{col}, T_{amb})GA \tag{12}$$

At steady state, this is balanced by the heat input to the sorption refrigerator which is given by

$$\dot{Q}_{sorption} = \frac{SCP(T_{col}, T_{amb})}{COP(T_{col}, T_{amb})} \tag{13}$$

For a given ambient temperature T_{amb} and solar insolation G, the collector temperature which gives the correct balance $\dot{Q}_{col} = \dot{Q}_{sorption}$ must be found. This is carried out in MATLAB® using the 'fminsearch' function minimisation routine and linear interpolation of the COP and SCP data from the sorption system model.

<u>Ice Production Calculation</u>

The quantity of ice produced was calculated using the following expression:

$$M_{ice} = \frac{Q_{cool}}{L_{water} + c_{pwater}(T_{amb} - 273)} \tag{14}$$

where M_{ice} is the mass of ice produced (kg), Q_{cool} is the cooling (J), L_{water} is the latent heat of fusion of water (taken as 335.5 kJ kg^{-1}) and c_{pwater} is the specific heat capacity of water (taken as 4200 J kg^{-1}K^{-1}).

<u>Weather Data</u>

Weather data for Dakar (Senegal) was obtained from the Meteonorm 4.0 package. The ambient temperature was taken as the air temperature and the solar insolation as the hemisphere radiation on a tilted plane. The solar collector was set South facing with an inclination equal to the latitude of 14°. **Figure 6** plots the monthly mean ambient temperature during operation of the system.

Results and Discussion

In **Figure 7**, the four combinations of collector and cycle type are compared on the basis of the annual mean daily mass of ice produced per square metre of collector area. The ratio of the collector area to the total mass of carbon adsorbent in the adsorption refrigerator is varied for each case and an optimum found which maximises the ice production per square metre of collector. The optimum ratio is 0.625 and 1.5 $m^2\ kg^{-1}$ for the two-bed and four-bed cycles, respectively.

Figure 8 plots the mean daily ice production for each month of the year with a four-bed cycle and the optimal area of evacuated tube collectors. It can be seen from the figure that the maximum ice production is in April at 13.7 kg m^{-2} and the minimum in July at 8.6 kg m^{-2}. Although the solar insolation is higher in July, the ambient temperature is also higher which reduces the performance of the adsorption refrigerator. This would have to be considered when sizing the machine along with the fact that the storage box itself will have higher losses at higher ambient temperatures and therefore require more cooling. This ice production is higher than the 4 to 7 kg m^{-2} reported by Wang and Oliveira [9] for state-of-the-art solar powered adsorption ice makers.

The optimum collector areas in **Figure 7** will only be optimal in terms of capital cost if the cost of the adsorption machine is negligible in comparison to that of the collector array. The cost of the adsorption machine is largely that of the sorption generators. Their cost has been calculated at €70 per kg of adsorbent, which is based on the cost of the plate heat exchanger in **Table 2** assuming the same cost per plate. The price given in **Table 2** is the retail price for a one-off unit and could be reduced if the systems were produced in large numbers. The sorption generator cost is then added to the solar collector cost from **Table 1** to obtain an estimate of the total cost.

Figure 9 shows the annual mean daily mass of ice produced per unit cost of the system. It can be seen from the figure that the four-bed system marginally outperforms the two-bed, producing 0.0147 kg of ice per day per € of total cost compared to 0.0129 kg/€ with evacuated tube collectors. However, in practise the greater complexity of the four-bed system may make the two-bed system favourable. Evacuated tube collectors prove more economic than flat plate collectors, their higher performance outweighing their higher capital cost. It can also be seen from **Figure 9** that the cost of the adsorption machine is only high enough to alter the optimum collector area in the case of flat plate collectors with a four-bed system.

The four-bed system with evacuated tube collectors would have a capital cost of €68,000 for a machine which could produce an average of 1000 kg of ice per day, consisting of €10,200 for the adsorption machine and €57,800 for 91 m^2 of evacuated tube collectors. Although still relatively high, the running costs would be extremely low and a lifetime of 20 years could be expected, which equates to an annual cost of €3,400.

Work is currently being performed to increase the thermal conductivity of the carbon adsorbent, which could further increase the SCP and reduce the cost of the adsorption machine. As solar collector technology develops and production quantities increase, their price will also reduce significantly.

Conclusions

The feasibility of applying a novel plate heat exchanger solid sorption generator to solar powered refrigeration for developing countries has been investigated. Computational modelling has predicted that for a four-bed adsorption system with evacuated tube collectors, an annual average daily ice production rate of 11 kg per square metre of collector could be achieved. The cost of a system which could produce up to 1000 kg of ice per day in Dakar (Senegal) has been estimated at €68,000.

References

[1] R.E. Critoph, S.J. Metcalf, Specific cooling power intensification limits in ammonia-carbon adsorption refrigeration systems, Applied Thermal Engineering, 24 (5-6) (2004), 661-678.

[2] R.E. Critoph, Heat Exchanger, UK Patent Application No 0617721.6 (2006).

[3] Z. Tamainot-Telto, S.J. Metcalf, R.E. Critoph, Novel compact sorption generators car air conditioning, International Journal of Refrigeration, 3 (4) (2009), 727-733.

[4] A. Diallo, Status of fish stocks in Senegal, in: E.K. Abban, C.M.V. Casal, T.M. Falk and R.S.V. Pullin (eds.), Biodiversity and Sustainable use of fish in coastal zone, pp. 38-40, 2000.

[5] Sustainable management of fish resources project: Senegal, The World Bank, Report No 45462-SN (2008).

[6] S. J. Metcalf, Compact high efficiency carbon-ammonia adsorption heat pump, University of Warwick, PhD Thesis (2009).

[7] W.M. Kays and A.L. London, Compact heat exchangers, McGraw-Hill Ed., 1984.

[8] R. E. Critoph, Evaluation of alternative refrigerant-adsorbent pairs for refrigeration cycles, Applied Thermal Engineering, 16 (11) (1996), 891-900.

[9] R.Z. Wang, R.G. Oliveira, Adsorption refrigeration – An efficient way to make good use of waste heat and solar energy, Progress in Energy and Combustion Science, 32 (2006), 424-458.

Table 1: Solar collector types, cost and performance data

Collector	**Type**	**Cost (€/m^2)**	**Optical efficiency, η_0**	**Linear loss coefficient, k_1 (W m^{-2}K^{-1})**	**Quadratic loss coefficient, k_2 (W m^{-2}K^{-2})**
Viessmann Vitosol 100 S2.5	Flat Plate	400	0.85	4.07	0.007
Thermomax Solamax 20 - TDS300	Evacuated Tube	636	0.769	1.61	0.0032

Table 2: Plate heat exchanger used in sorption system cost estimates

Heat Exchanger Type	**Cost (€)**	**Plate Size (m)**	**Plate area (m^2)**	**No of plates**	**Cost per plate (€)**
UK Heat Exchangers SL23TL-AA-40	€220	0.312×0.076	0.0237	40	€5.5

Table 3: Modelled sorption generator parameters

Parameter	**Value**	**Unit**
Carbon type	Chemviron Carbon SRD1352/3	-
Carbon thickness, t_c	4	mm
Carbon conductivity, k_c	0.3	W $m^{-1}K^{-1}$
Carbon density	435	kg m^{-3}
Limiting NH_3 mass concentration, x_0	0.5691	kg kg^{-1}
D-A equation coefficient k	6.6738	
D-A equation exponent n	1.1489	
Fluid channel depth, t_f	0.5	mm
Wall thickness, t_w	0.15	mm
Wall material	316 Stainless Steel	
Heat transfer Fluid	Mineral Oil	-
Heat transfer fluid density	800	kg m^{-3}
Heat transfer fluid thermal conductivity	0.14	W $m^{-1}K^{-1}$
Heat transfer fluid specific heat capacity	2300	J $kg^{-1}K^{-1}$

Figure 1: Prototype plate heat exchanger sorption generator

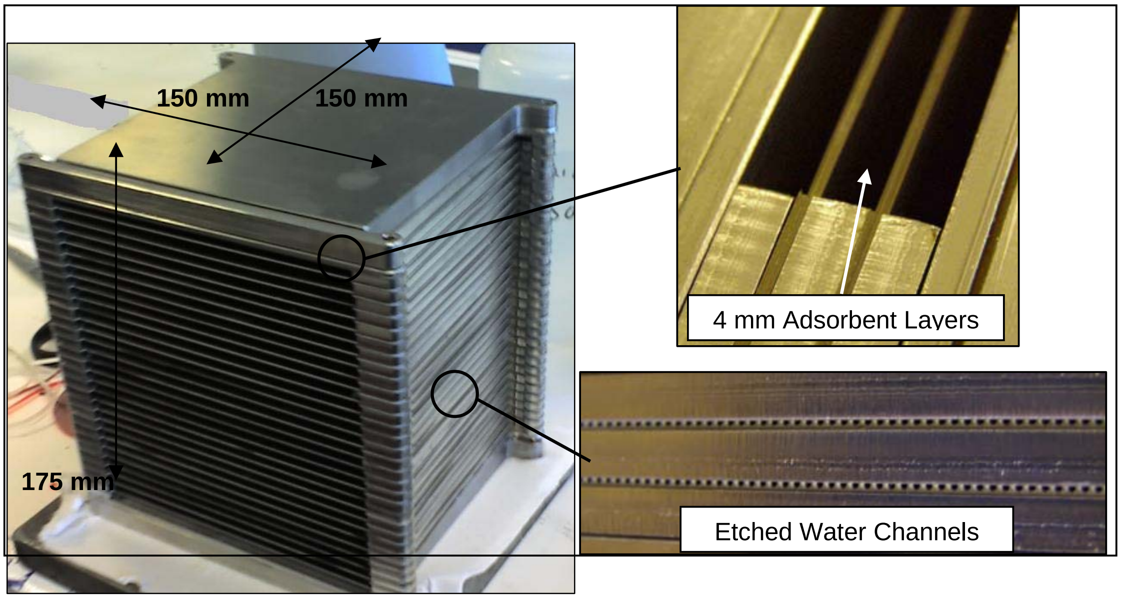

Figure 2: Layout of a solar powered sorption refrigeration system (with two beds)

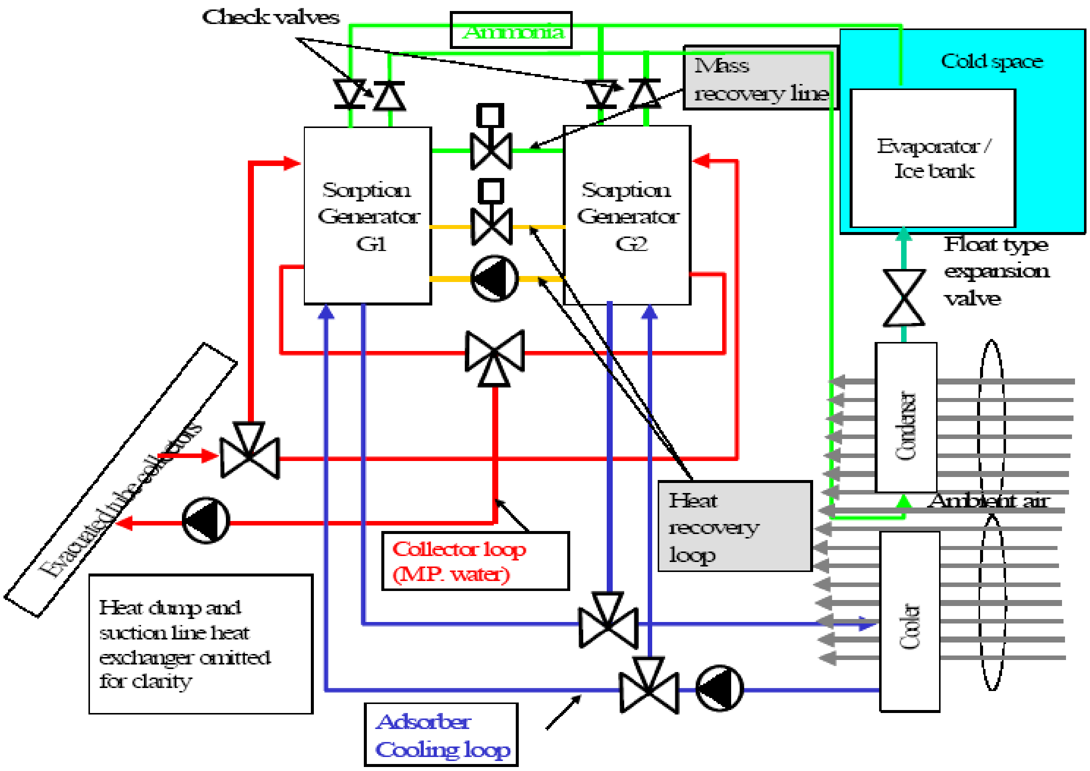

Figure 3: Schematic diagram of the sorption generator finite difference model

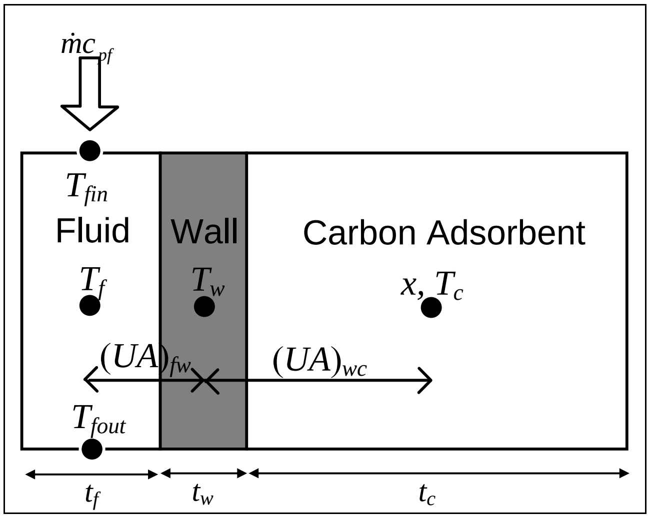

Figure 4: Two-bed cycle sorption system performance

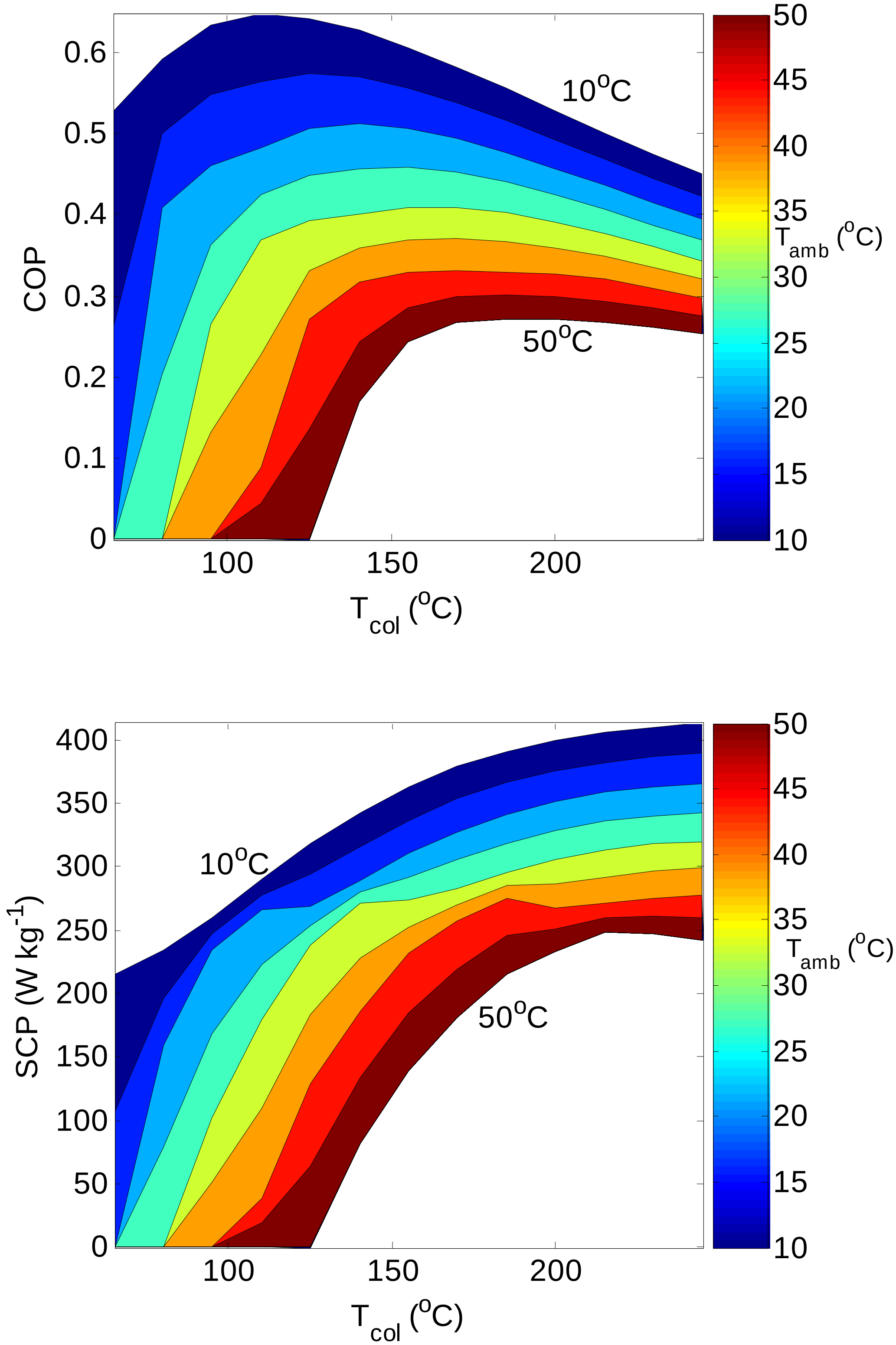

Figure 5: Four-bed cycle sorption system performance

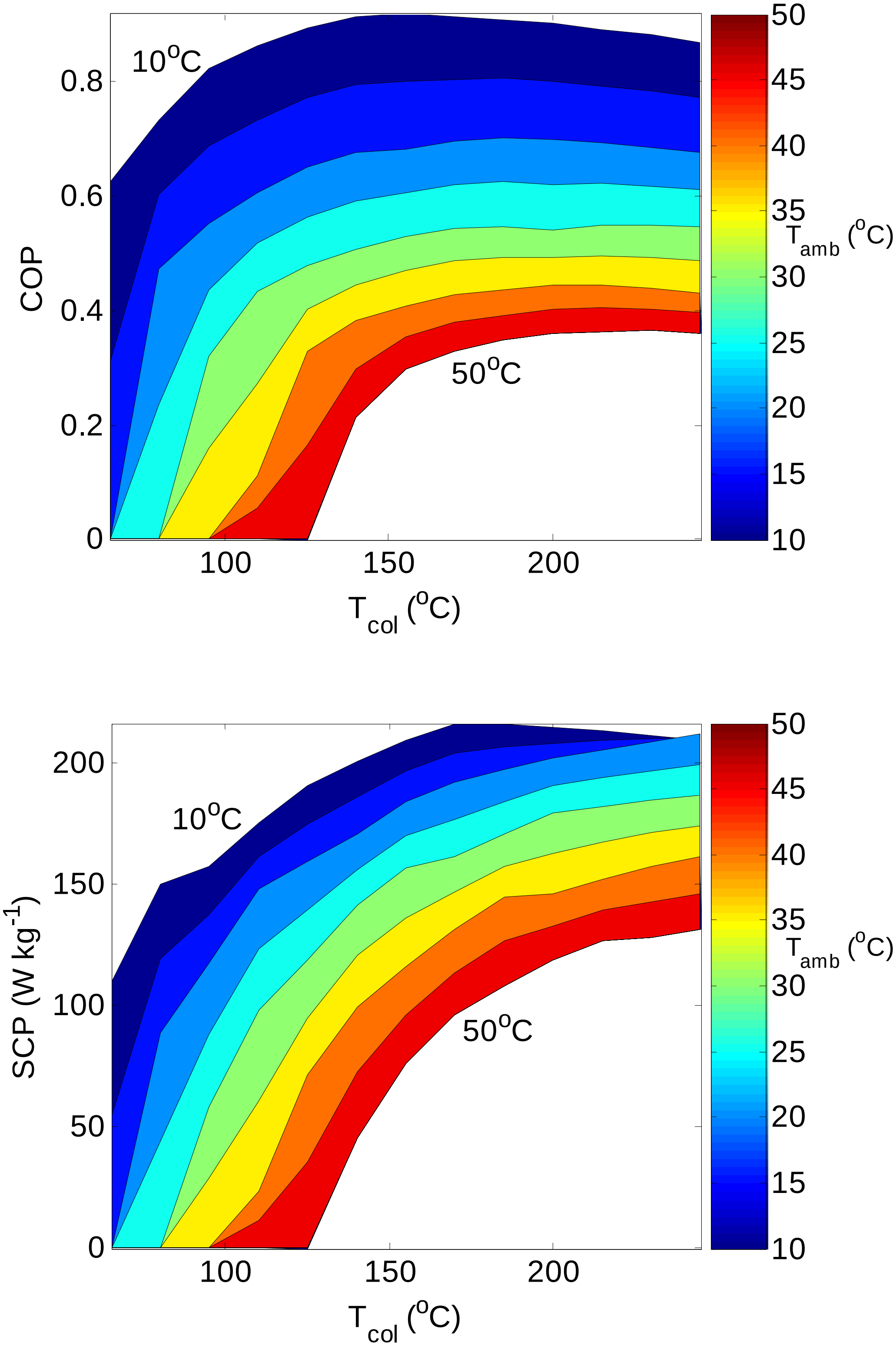

Figure 6: Monthly mean ambient temperature for Dakar, Senegal

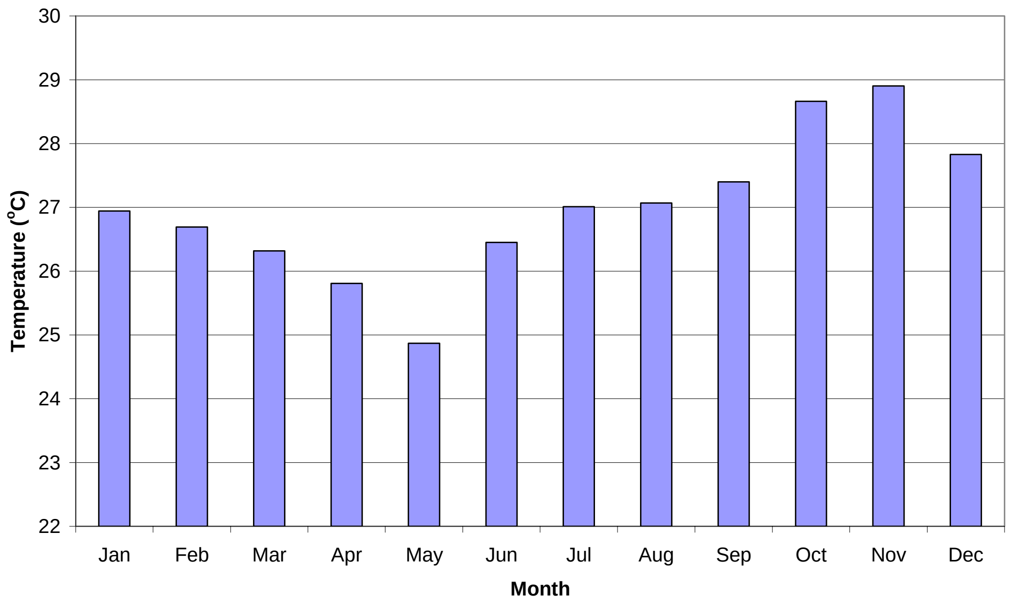

Figure 7: Annual mean daily ice production for the four combinations of collector and cycle type.

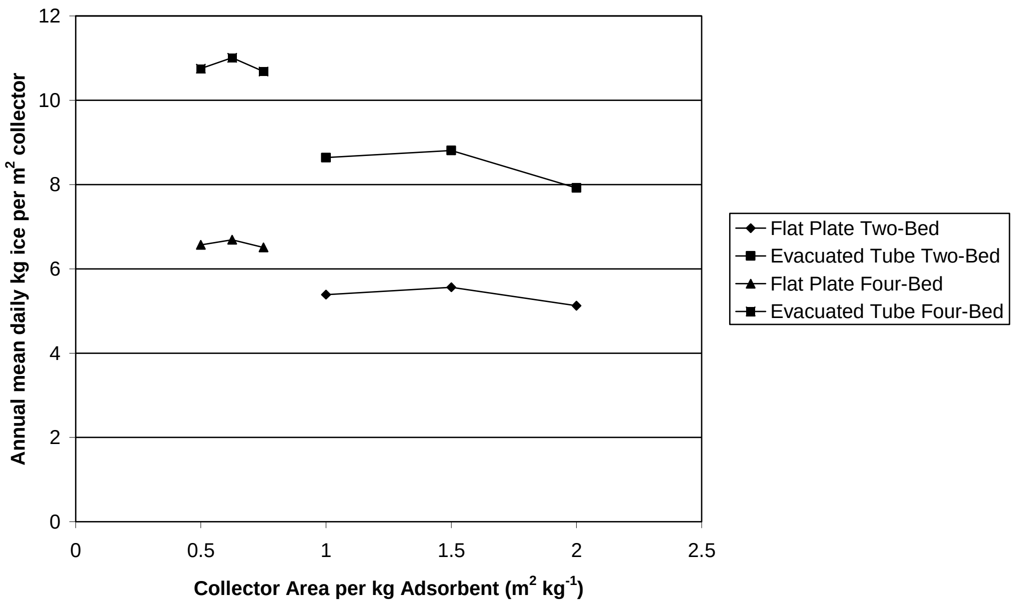

Figure 8: Mean daily ice production for each month with a four-bed cycle and evacuated tube collectors

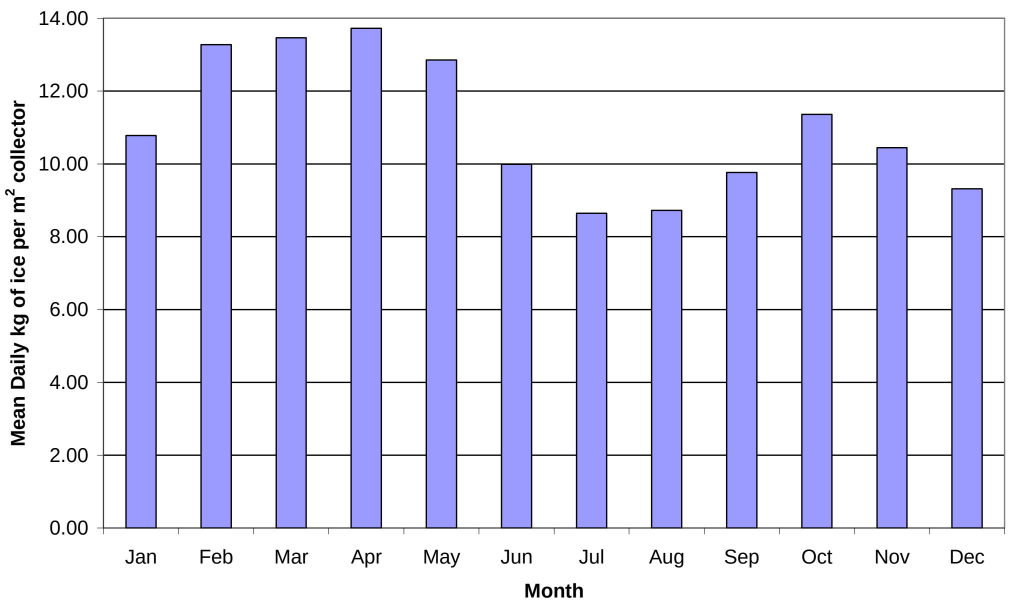

Figure 9: Daily ice production per unit total system cost